IEEE Access
Multidisciplinary | Rapid Review | Open Access Journal

Received December 23, 2020, accepted January 4, 2021, date of publication January 8, 2021, date of current version January 19, 2021.

Digital Object Identifier 10.1109/ACCESS.2021.3050235

Analysis of the Capture Rate of Barrel Weapon Test Based on Laser Screen Velocity Measurement System

TAO DONG[1], JIUQI YANG[1], DING CHEN[2], (Member, IEEE), AND LINGQIU TAN[3]

[1]Shaanxi Province Key Laboratory of Photoelectric Measurement and Instrument Technology, Xi'an Technological University, Xi'an 710021, China
[2]School of Armament Science and Technology, Xi'an Technological University, Xi'an 710021, China
[3]School of Optoelectronic Engineering, Xi'an Technological University, Xi'an 710021, China

Corresponding author: Jiuqi Yang (yang197@outlook.com)

This work was supported in part by the Young Scientists Fund of the National Natural Science Foundation of China under Grant 61905187, in part by the National Natural Science Foundation in Shaanxi Province of China under Grant 2019JM-238, and in part by the Scientific Research Program funded by Shaanxi Provincial Education Department under Grant 20JS059.

ABSTRACT The flying velocity is a key parameter of the projectile in the exterior ballistic test, which is usually measured by the laser screen velocity measurement system. However, how to set the system parameters reasonably to ensure the system capture rate is a challenge due to the insufficient research. In order to solve this problem, our research reveals the change law of the system capture rate by deriving the mathematical model and simulation based on the principle of system detection and the gun firing distribution law. With the three system settings in the simulation, the critical height of the muzzle are 3.78m, 4.1m, and 3.9m respectively. Within the critical height, the system capture rate is greater than 99% theoretically. If it exceeds the critical height, the system capture rate will drop rapidly to 0. In addition, changing the laser power or the arrangement of the detection devices during the test will affect the system capture rate. To verify the simulation result, we perform a gun shoot experiment, fully confirming our analyses.

INDEX TERMS Photoelectric detection, projectile velocity measurement, laser screen, analysis of detection performance.

I. INTRODUCTION

Projectile velocity is an important parameter for evaluating the performance of barrel weapons such as firearms and guns [1]–[6], photoelectric detection using laser screen velocity measurement system has emerged as a powerful technique for measuring projectile velocity in the exterior ballistic test. The system is depended on the zone-block measurement method, which is two detection devices with photoelectric induction areas are perpendicular to the trajectory line, and when a projectile passes through their detection area, two induction signals will be generated. The time interval between two signals is measured by a chronometer, and the projectile velocity is calculated according to the distance of two devices divided by the time [7]–[15]. However, the system detection performance decreases with ballistic height, and projectiles may be higher than the effective detection range of the system due to firing random dispersion, which is a challenging problem. Therefore, how to reveal the change law of system capture rate and reasonably set system parameters to ensure effective capture of target in test is now arousing exploration.

Many researchers introduced the detection principle and measurement errors of the system, but there were few studies on the analysis of the system capture rate [7], [8], [10]–[12]. Tian, Hui, *et al.* studied the sensitivity of an LED light screen velocity measurement system with large detection area, but did not further study its capture rate [13]. Wang Fan, *et al.* analyzed the laser energy attenuation law of the laser screen system used for underwater target velocity measurement, whereas they did not explore how it affects the system capture rate [14]. Li Hanshan, *et al.* established the capture rate model of a passive photoelectric velocity measurement system, but the system used natural light for detection, its anti-interference ability is poor [15]. Laser screen velocity measurement system has the advantages of high sensitivity and strong anti-interference ability [12], [16], but the lack of analysis of its capture rate at present has an adverse effect on its application. Therefore, we deduced the system capture rate model, based on the detection principle of the laser screen

The associate editor coordinating the review of this manuscript and approving it for publication was Bo Pu.

velocity measurement system, and factors such as the relative position of the system and the barrel weapon muzzle and the shooting angle of the barrel weapon in the test. We explored the change rule of the system capture rate through simulation calculation, and verified it by experiment.

II. SYSTEM DETECTION PRINCIPLE

As can be seen in Figure 1, the system detection device includes a laser, a Fresnel Lens, an optical filter, a slit diaphragm, a photodetector, and a central processing circuit. The laser generates a thin fan-shaped detection screen. When a projectile passes through a laser screen formed by the device, some reflected light by the projectile produces an increase in the energy falling on the photodetector, which makes the circuit output a response signal. If two or more devices are deployed on the preset trajectory, the time interval will be obtained by the electrical chronometer between the signals, and by processing and calculating, the velocity or other parameters of the projectile will be acquired.

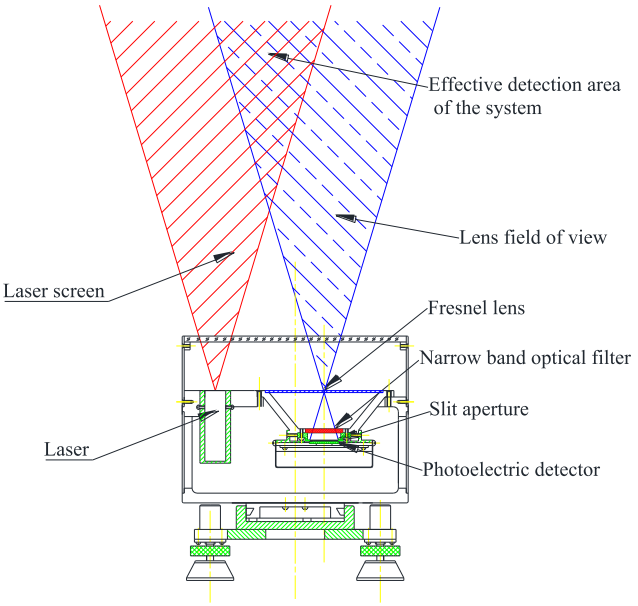

FIGURE 1. The schematic diagram of the laser screen velocity measurement system.

It is illustrated in Figure 2 that the effective detection area of the system and the coordinates settings. The principal point O of the lens is the origin, and the coordinate of the laser emitting point P is $(x_P, 0)$.

For simplicity, the projectile is assumed to be an ideal cylinder with diameter d and length l. The coordinate of the impact point E is (x, y), that is, the distance between the impact point and the optical axis of the lens is $|x|$, and the ballistic height is y. According to the detection principle and references [13]–[16], the signal amplitude V when the projectile with caliber d passes the laser screen is as follows:

$$V = \frac{\varepsilon RGD^2 d\rho\eta P_0}{8\theta\left(x^2+y^2\right)\sqrt{(x-x_P)^2+y^2}} \tag{1}$$

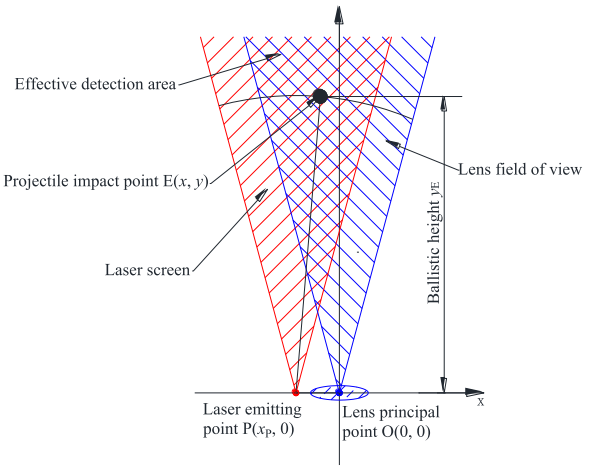

FIGURE 2. The effective detection area of the system.

where ε is the responsivity of the photodetector, R is the feedback resistance of the circuit, G is the circuit magnification, D is the effective aperture of the system optical lens, ρ is the spectral reflectance of the projectile surface, η is the transmittance of the optical filter, P_0 is the output power of the laser, θ is the effective field of view angle of the lens and the divergence angle of the laser screen.

In order to filter some noises, the signal trigger threshold V_m is usually set, and when $V > V_m$, the chronometer can be triggered to realize the detection of the projectile. Therefore, if the system parameters such as P_0 and θ are constant, when d, y, and x satisfy the following relationship, the projectile can be detected.

$$\frac{\varepsilon RGD^2 d\rho\eta P_0}{8\theta\left(x^2+y^2\right)\sqrt{(x-x_P)^2+y^2}} > V_m \tag{2}$$

III. SYSTEM CAPTURE RATE MODEL

In the projectile velocity measurement of firearms, guns and other barrel weapons, horizontal ballistic shooting and small angle shooting are commonly used test layouts [17], [18]. Since projectiles generally have very high velocity, they are usually considered to be uniform linear motions between the detection area of the two zone-block devices (They can be called device-1 and device-2).

When shooting at a small angle of fire, angle of fire and azimuth have a more obvious impact on the ballistic performance.

Firing angle θ_a equals to the sum of elevation angle τ of muzzle before shooting and longitudinal jump angle τ_J. Azimuth angle θ_b is equal to the sum of azimuth angle ψ of the muzzle before shooting and lateral jump angle ψ_J. θ_a and θ_b are as follows

$$\theta_a = \tau + \tau_J \tag{3}$$

$$\theta_b = \psi + \psi_J \tag{4}$$

From the analysis of exterior ballistics, it is known that influencing factors of jump angle are mostly random variables, which make jump angle obey a certain distribution.

Generally, τ_J and ψ_J are treated as Gaussian distribution, namely $\tau_J \sim N(\mu_{\tau J}, \sigma^2_{\tau J})$, $\psi_J \sim N(\mu_{\psi J}, \sigma^2_{\psi J})$, and their probability density functions are as follows:

$$f_{\tau_J}(\tau_J) = \frac{1}{\sqrt{2\pi}\sigma_{\tau_J}} e^{-\frac{(\tau_J-\mu_{\tau_J})^2}{2\sigma^2_{\tau_J}}} \tag{5}$$

$$f_{\psi_J}(\psi_J) = \frac{1}{\sqrt{2\pi}\sigma_{\psi_J}} e^{-\frac{(\psi_J-\mu_{\psi_J})^2}{2\sigma^2_{\psi_J}}} \tag{6}$$

As shown in Figure 3(a), we take the projectile velocity test of the horizontal firing gun as an example for analysis. Figure 3(b) shows the geometric coordinate relationship of the test system. The principal point $O^{(1)}$ of the lens of the detecting device-1 is set the coordinate origin O. The detection screen of device-1 is in the xOy plane, and the detection screen of device-2 is parallel to the xOy plane. $O^{(2)}(0, 0, z_{O-2})$ is the principal point of the lens of the detection device-2. $P^{(1)}$, $P^{(2)}$ are the laser emitting points of the detection device-1 and device-2 respectively, and the muzzle center point is G. The predetermined trajectory is L_{BP}, which is parallel to the z axis and the actual trajectory is L_{BA}. The intersection points of L_{BP}, L_{BA} and the detection screen of the device-1 are $E_P^{(1)}$, $E_A^{(1)}$, and the intersection points of L_{BP}, L_{BA} and the effective detection screen of the device-2 are $E_P^{(2)}$, $E_A^{(2)}$.

The distance between the two detection screens is L_M, and the distance between the muzzle and the detection screen of device-1 is L_G. $x_{EA}^{(1)}$ and $y_{EA}^{(1)}$ are abbreviated as x_1 and y_1

$$x_1 = x_G + L_G \tan\psi_J \tag{7}$$

$$y_1 = y_G + L_G \tan\tau_J \tag{8}$$

Since value ranges of τ_J and ψ_J are both within $(-\pi/2, \pi/2)$, the probability density functions of x_1 and y_1 are respectively

$$f_x(x_1) = f_{\psi_J}[h(x_1)]\left|h'(x_1)\right| \tag{9}$$

$$f_y(y_1) = f_{\tau_J}[h(y_1)]\left|h'(y_1)\right| \tag{10}$$

In the above two formulas, $h(x_1)$, $h'(x_1)$, $h(y_1)$, $h'(y_1)$ are

$$h(x_1) = \arctan\left(\frac{x_1 - x_G}{L_G}\right) \tag{11}$$

$$h'(x_1) = \frac{1}{1+\left(\frac{x_1-x_G}{L_G}\right)^2} \cdot \frac{1}{L_G} \tag{12}$$

$$h(y_1) = \arctan\left(\frac{y_1 - y_G}{L_G}\right) \tag{13}$$

$$h'(x_1) = \frac{1}{1+\left(\frac{x_1-x_G}{L_G}\right)^2} \cdot \frac{1}{L_G} \tag{14}$$

So $f_{x1}(x_1), f_{y1}(y_1)$ are

$$f_{x1}(x_1) = \frac{1}{\sqrt{2\pi}\sigma_{\psi_J}} e^{-\frac{\left[\arctan\left(\frac{x_1-x_G}{L_G}\right)-\mu_{\psi_J}\right]^2}{2\sigma^2_{\psi_J}}} \cdot h'(x_1) \tag{15}$$

$$f_{y1}(y_1) = \frac{1}{\sqrt{2\pi}\sigma_{\tau_J}} e^{-\frac{\left[\arctan\left(\frac{y_1-y_G}{L_G}\right)-\mu_{\tau_J}\right]^2}{2\sigma^2_{\tau_J}}} \cdot h'(y_1) \tag{16}$$

If the signal amplitude V generated by the projectile passing through the laser screen is greater than threshold V_m, the chronograph will be triggered. We consider that the firing dispersion will not exceed the left and right boundaries of the effective detection area of the devices, so the distribution function $F_V(u)$ satisfied by V is

$$F_V(u) = \int\int_{V(x_1,y_1)<u} f_{x_1}(x_1) f_{y_1}(y_1) dx_1 dy_1 \tag{17}$$

The probability of device-1 detecting the target Γ_1 (that is, the probability that V_1 is greater than the threshold V_m) is

$$\Gamma_1 = \Gamma\{V(x_1, y_1) > V_m\} = 1 - \Gamma\{V(x_1, y_1) < V_m\} \tag{18}$$

Therefore, the following formula can be deduced

$$\Gamma_1 = 1 - \int\int_{V(x_1,y_1)} f_{x_1}(x_1) f_{y_1}(y_1)\, dx_1 dy_1 \tag{19}$$

Similarly, the probability Γ_2 of detecting the target by device-2 is

$$\Gamma_2 = 1 - \int\int_{V(x_2,y_2)} f_{x_2}(x_2) f_{y_2}(y_2)\, dx_2 dy_2 \tag{20}$$

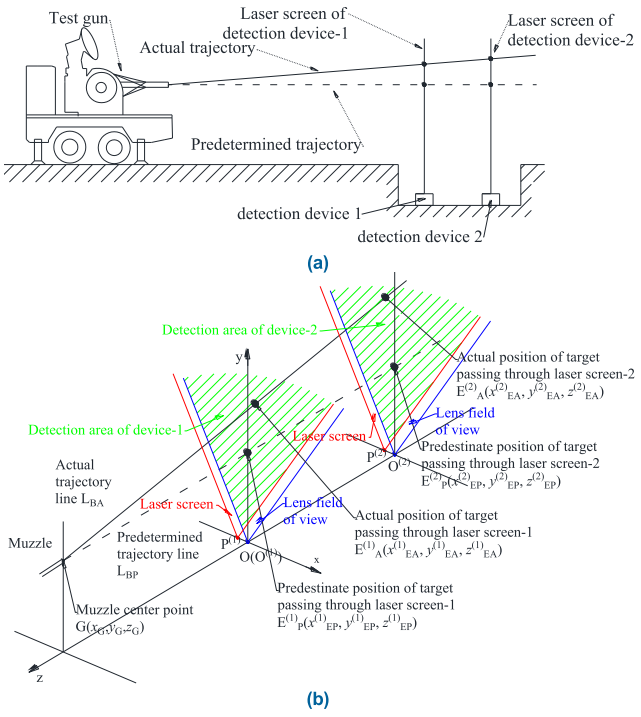

FIGURE 3. Projectile velocity test of gun horizontal firing using two detection devices, (a) Diagram of gun trajectory dispersion, (b) Definition of test coordinate system.

In summary, we express the probability Γ that the system detects the target as

$$\begin{aligned}\Gamma &= \Gamma_1 \cdot \Gamma_2 \\ &= \left(1 - \int\int_{V(x_1,y_1)<V_m} f_{x_1}(x_1) f_{y_1}(y_1)\, dx_1 dy_1\right) \\ &\quad \times \left(1 - \int\int_{V(x_2,y_2)<V_m} f_{x_2}(x_2) f_{y_2}(y_2)\, dx_2 dy_2\right) \end{aligned} \quad (21)$$

The final expression relates the system capture rate to parameters of system and layout. In addition, in the actual test, because the projectile is affected by gravity during the flight, it is necessary to consider the correction of projectile coordinates.

IV. SYSTEM CAPTURE RATE SIMULATION ANALYSIS

Following the analysis of the mathematical model, we knew the system capture rate was related to the muzzle position, preset trajectory, shooting dispersion size, and relative position of the detection devices. We simulated the capture rate of the system for the horizontal firing projectile velocity test of a 30mm rapid-fire gun, the system layout and the establishment of the coordinate system were the same as those in Figure 3. The muzzle was 50m away from the detection screen of the device-1, and the distance between the two devices was 10m. According to the experimental data of exterior ballistics, the mean value and standard deviation of the longitudinal jump angle τ_J and the lateral jump angle ψ_J during automatic shooting are shown in Table 1. In addition, the simulation parameters of the detection system are shown in Table 2.

TABLE 1. Gun firing dispersion parameters.

	The mean value	The standard deviation
The longitudinal jump angle τ_J	0.2318	0.01891
The lateral jump angle ψ_J	0.0814	0.01201

We used the parameters of the gun jump angle and the law of external ballistic movement to obtain the probability density diagrams of projectiles spreading on the plane of laser screen-1 and laser screen-2 as shown in Figure 4(a) and Figure 4(b) (Here, the muzzle height z_G was set to 2m, and for other muzzle heights, the probability function was only translated without the shape changed.).

The relationship between Γ, Γ_1, Γ_2 and the muzzle height z_G was obtained from the simulation as shown in Table 3.

From Table 3, the simulation results was seen that when the muzzle is 50m away from the detection screen of the device-1, the distance between the two devices was 10m, and the muzzle height z_G is less 3.75m, the capture rate of the two devices and the system were all equal to 1. As the muzzle height

TABLE 2. The system parameters of the simulation.

Symbol	Parameter	Value
d	Projectile caliber	30mm
ε	Responsivity of detector	0.6A/W
G	Circuit magnification	120
R	Circuit feedback resistance	50kΩ
D	Effective aperture of lens	0.12m
f	Focal length	50mm
η	Filter transmittance	0.75
P_0	Laser power	800mW
λ	Laser wavelength	780nm
$(x_P, 0)$	Position of laser emission point	(−0.1m, 0)
b	Thickness of laser screen	4mm
θ	Divergence angle of laser screen	30°
θ_v	Effective field angle of lens	30°
ρ	Surface reflectance of projectile	0.6

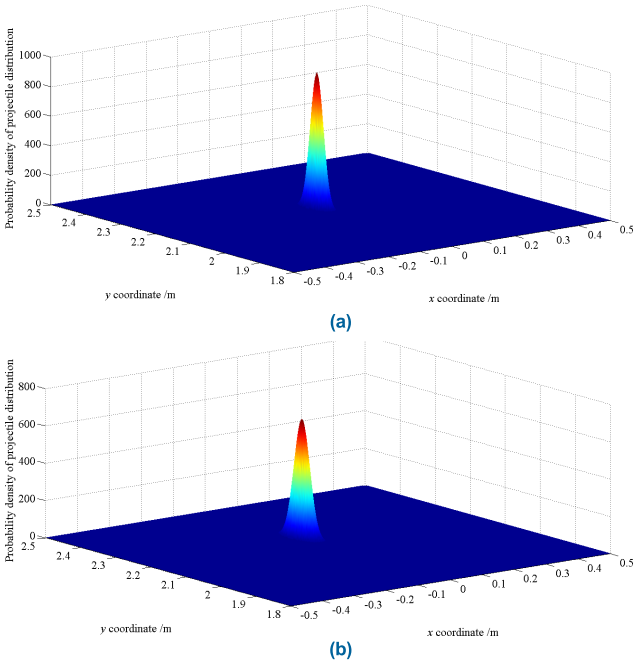

FIGURE 4. The probability distribution of the projectile at the detection laser screens when the muzzle height z_G is 2m, (a) The probability distribution at the laser screen of device-1, (b) The probability distribution at the laser screen of device-2.

continued to increase, the capture rate of device-2 and device-1 decreased successively, which led to a sharp decrease in the system capture rate. If the muzzle height z_G exceeded 3.90m, the system capture rate became 0. Therefore, it demonstrated that the critical height of the muzzle with a test capture rate greater than 99% was 3.78m theoretically. In the actual test, the muzzle height z_G should be less than 3.78m to ensure the system capture rate.

Next, we increased the laser power of the two devices to 1.2W, and the relationship between the capture rate and the muzzle height z_G became as shown in Table 4.

Our simulation results demonstrated that when the laser power of the two detection devices was increased to 1.2W and the muzzle height z_G is less than 4.30m, the capture rate

TABLE 3. The capture rate varies with muzzle height.

The muzzle height z_G /m	Capture rate of detection device-1 Γ_1	Capture rate of detection device-2 Γ_2	System capture rate Γ
<3.75	1.0000	1.0000	1.0000
3.75	1.0000	1.0000	1.0000
3.76	1.0000	0.9999	0.9999
3.77	1.0000	0.9992	0.9992
3.78	1.0000	0.9960	0.9960
3.79	1.0000	0.9842	0.9842
3.80	1.0000	0.9500	0.9500
3.81	0.9998	0.8728	0.8726
3.82	0.9981	0.7372	0.7358
3.83	0.9887	0.5517	0.5455
3.84	0.9530	0.3539	0.3373
3.85	0.8575	0.1895	0.1625
3.86	0.6784	0.0831	0.0564
3.87	0.4433	0.0294	0.0130
3.88	0.2271	0.0083	0.0019
3.89	0.0878	0.0019	0.0002
3.90	0.0250	0.0000	0.0000
>3.90	<0.005	0.0000	0.0000

TABLE 4. The capture rate varies with muzzle height (The laser power increased to 1.2W).

The muzzle height z_G /m	Capture rate of detection device-1 Γ_1	Capture rate of detection device-2 Γ_2	System capture rate Γ
<4.30	1.0000	1.0000	1.0000
4.30	1.0000	0.9999	0.9999
4.31	1.0000	0.9995	0.9995
4.32	1.0000	0.9972	0.9972
4.33	1.0000	0.9884	0.9884
4.34	1.0000	0.9612	0.9612
4.35	1.0000	0.8961	0.8961
4.36	1.0000	0.7748	0.7748
4.37	1.0000	0.5986	0.5986
4.38	1.0000	0.3993	0.3993
4.39	1.0000	0.2236	0.2236
4.40	0.9996	0.1030	0.1030
4.41	0.9968	0.0384	0.0383
4.42	0.9829	0.0115	0.0113
4.43	0.9348	0.0027	0.0025
4.44	0.8177	0.0000	0.0000
4.45	0.6182	0.0000	0.0000
>4.45	0.3802	0.0000	0.0000

of the two devices and the system were all equal to 1. As the muzzle height continued to increase, the capture rate of the two devices began to decrease, which caused a decrease in the system capture rate. When the muzzle height z_G exceeded 4.44m, the system capture rate became 0. Therefore, under this setting, the critical height of the muzzle was 4.32m. Compared with Table.3, it was concluded that increasing the laser power can increase the critical height of the muzzle that ensured the test capture rate was greater than 99%.

We kept the system parameters the same as that of the first simulation, and changed the system layout as the distance between the muzzle and the detection screen of device-1 was 20m, and the distance between the two devices was 10m. The simulation results are shown in Table 5.

TABLE 5. The capture rate varies with muzzle height (after layout change).

The muzzle height z_G /m	Capture rate of detection device-1 Γ_1	Capture rate of detection device-2 Γ_2	System capture rate Γ
<3.90	1.0000	1.0000	1.0000
3.90	1.0000	1.0000	1.0000
3.91	1.0000	0.9990	0.9990
3.92	1.0000	0.9818	0.9818
3.93	1.0000	0.8607	0.8607
3.94	1.0000	0.5294	0.5294
3.95	1.0000	0.1746	0.1746
3.96	0.9977	0.0258	0.0257
3.97	0.9072	0.0016	0.0015
3.98	0.4243	0.0001	0.0000
3.99	0.0440	0.0000	0.0000
4.00	0.0007	0.0000	0.0000
4.01	0.0000	0.0000	0.0000
4.02	0.0000	0.0000	0.0000
4.03	0.0000	0.0000	0.0000
4.04	0.0000	0.0000	0.0000
4.05	0.0000	0.0000	0.0000
>4.05	0.0000	0.0000	0.0000

We obtained the following results with the system layout changed. When the muzzle height z_G is less than 3.90m, the capture rate of the two devices and the system are all 1. The capture rate of the two devices decreased successively with the muzzle height continued to increase, which made the system capture rate drop. When the muzzle height z_G exceeded 3.98m, the system capture rate became 0. For that, the critical height of the muzzle was 3.91m. Compared with Table 3, it was seen that the change in the arrangement of the detection devices affected the change in the system capture rate. Specific changes need to be calculated based on the capture rate model.

V. EXPERIMENT

Experiments were conducted using the 30mm rapid-fire gun described in the simulation section. The system parameters of the detection devices were the same as those in Table 2. We performed three groups of experiments with different system parameters and layouts, corresponding to the simulation section. In each group of experiments, we controlled the gun to shoot at the set ballistic height and record the capture rate of the system.

Table 6 displays the experimental results when the muzzle is 50m away from the detection screen of the device-1, and the distance between the two devices is 10m.

It was seen from the simulation section that under this arrangement, the critical trajectory height of the experimental gun was 3.78m, that is, when the trajectory height was less than 3.78m, the system capture rate was greater than 99%, and as the trajectory height continued to increase, the system capture rate suddenly decreased until it was 0. According to the results of the experiment, the system capture rate was

TABLE 6. The experimental data of first group.

Muzzle height zG /m	Number of projectiles fired	Capture rate of device-1 Γ_1	Capture rate of device-2 Γ_2	System capture rate Γ
3.50	10	100%	100%	100%
3.60	10	100%	100%	100%
3.70	10	100%	100%	100%
3.80	10	100%	90%	90%
3.90	10	0%	0%	0%

Experimental conditions: no rain, snow and fog, ground longitudinal and cross wind speed is less than 4m/s

100% when 10 projectiles were fired at the ballistic height of 3.50m, 3.60m and 3.70m respectively. However, when the ballistic height was 3.90m, the 10 projectiles could not be detected by the the two devices, and the system capture rate was 0%, which indicated that the system capture rate dropped sharply in a part range from 3.70m to 3.90m. It was consistent with the theoretical analysis of the change law of the capture rate, which verified the conclusion of the theoretical analysis of the capture rate model.

The experimental results of increasing the laser power to 1.2W are shown in Table 7.

TABLE 7. The experimental data of second group.

Muzzle height zG /m	Number of projectiles fired	Capture rate of device-1 Γ_1	Capture rate of device-2 Γ_2	System capture rate Γ
4.10	10	100%	100%	100%
4.20	10	100%	100%	100%
4.30	10	100%	100%	100%
4.40	10	100%	0%	0%
4.50	10	0%	0%	0%

Experimental conditions: no rain, snow and fog, ground longitudinal and cross wind speed is less than 4m/s

As known from the previous section, when the system laser increased to 1.2W, the critical ballistic height of the experimental gun was 4.32m, that is, when the ballistic height was less than 4.32 meters, the system capture rate was more than 99%. If the ballistic height continued to increase, the system capture rate dropped sharply until it was 0. Upon the experimental results, it was known that the system capture rate was 100% when shooting 10 projectiles at 4.10m, 4.20m and 4.30m, and 0% for 4.40m and 4.50m respectively. It was seen that that the capture rate of the system dropped sharply from 4.30m to 4.40m, which was consistent with the simulation results. In addition, compared with the first group of experiments, it was recognized that the detection performance of the system was improved with the increase of laser power.

In the third group of experiments, the layout of the first group of the experiment was changed to 20m between the muzzle and the detection screen of device-1, and the distance between the two devices was 10m, and the others parameters remained. The experimental results are shown in Table 8.

When the changed experimental layout was adopted, the critical trajectory height was 3.91m as shown from

TABLE 8. The experimental data of third group.

Muzzle height zG /m	Number of projectiles fired	Capture rate of device-1 Γ_1	Capture rate of device-2 Γ_2	System capture rate Γ
3.70	10	100%	100%	100%
3.80	10	100%	100%	100%
3.90	10	100%	100%	100%
4.00	10	0%	0%	0%
4.10	10	0%	0%	0%

Experimental conditions: no rain, snow and fog, ground longitudinal and cross wind speed is less than 4m/s

the simulation. If the ballistic height continued to increase, the system capture rate dropped sharply until it reached zero. We knew from the experimental results that the system capture rate of 10 projectiles fired at 3.70m, 3.80m and 3.90m were all 100%, while the capture rate of 10 projectiles fired at 4.00m and 4.10m were both 0%. The experimental results confirmed from 3.90m to 4.00m the capture rate of the system dropped to 0, which was consistent with the simulation results. In addition, compared with the first group of experiments, it could be seen that the detection performance of the system changed slightly with the change of experimental arrangement.

Overall considering the experimental results, we believed that the following conclusions could hold. With all the parameters and the experimental layout determined, the system had a critical trajectory height, which could be calculated by the capture rate model. When the muzzle height was below the critical height, the system capture rate was regarded as 100%, and if the muzzle height exceeded the critical height, the system capture rate dropped suddenly to zero. In addition, changing the laser power of the detection devices or the experimental arrangement would affect the system capture rate. In order to ensure a better capture rate, the ballistic height is generally selected below the critical height in practical application.

VI. CONCLUSION

In this paper, the analysis of the capture rate of barrel weapons test based on laser screen velocity measurement system is investigated. Based on the principle of system detection, the change law of the system capture rate is explored by establishing the capture rate model. Simulations suggest that in the three system settings, the critical ballistic height of muzzle are 3.78m, 4.32m and 3.91m respectively. When the muzzle height does not exceed the critical height, the test capture rate is more than 99%. If the critical height is exceeded, the system capture rate will drop to 0 sharply. Moreover, laser power and experimental arrangement also affect the capture rate of the system, and the specific changes can be calculated by the capture rate model. Finally, the trend of the capture rate with the ballistic height is verified through the three groups experiments. This can provide a good theory basis for improving the detection performance. In engineering application, the system can be adjusted according to the

specific requirements to ensure that the capture rate meets the relevant test requirements. For future research, we will focus on the system capture rate with more complex test layout, and further research is under discussion.

REFERENCES

[1] Z. Deng, Q. Shen, J. Cheng, and H. Wang, "Trajectory estimation method of spinning projectile without velocity input," *Measurement*, vol. 160, Aug. 2020, Art. no. 107831.
[2] E. Owlia and S. A. Mirjalili, "The effect of launcher parameters on the projectile velocity in laboratory electromagnetic weft insertion system," *J. Textile Inst.*, vol. 51, pp. 1–8, Aug. 2020.
[3] Y. Wang, T. Ma, D. Pei, C. Chen, K. Feng, D. Zhang, and Z. Wu, "Influence of magnetically confined plasma on the muzzle velocity of gun projectile," *IEEE Access*, vol. 8, pp. 72661–72670, 2020.
[4] S. G. Savio and V. Madhu, "Ballistic performance evaluation of ceramic tiles with respect to projectile velocity against hard steel projectile using DOP test," *Int. J. Impact Eng.*, vol. 113, pp. 161–167, Mar. 2018.
[5] Y. D. Zhang, Z. C. Lu, and H. M. Wen, "On the penetration of semi-infinite concrete targets by ogival-nosed projectiles at different velocities," *Int. J. Impact Eng.*, vol. 129, pp. 128–140, Jul. 2019.
[6] J. Liu, C. Wu, J. Li, Y. Su, and X. Chen, "Numerical investigation of reactive powder concrete reinforced with steel wire mesh against high-velocity projectile penetration," *Construct. Building Mater.*, vol. 166, pp. 855–872, Mar. 2018.
[7] H. Li, X. Zhang, X. Zhang, and L. Lu, "Model optimization and calculation method of multi-target curved motion parameters measurement using multi-screen intersection test mechanism," *IEEE Access*, vol. 8, pp. 147872–147879, Aug. 2020.
[8] Z. Wu, J. Ma, X. Zhang, and J. Ni, "Research on accurate calibration method of screen plane equation of sky screen vertical target," *Optik*, vol. 174, pp. 86–90, Dec. 2018.
[9] W. Chu, D. Zhao, B. Liu, B. Zhang, and Z. Gui, "Research on target deviation measurement of projectile based on shadow imaging method in laser screen velocity measuring system," *Sensors*, vol. 20, no. 2, pp. 1–16, 2020.
[10] H. Li, "Multi-target space position identification and matching algorithm in multi-screen intersection measurement system using information constraint method," *Measurement*, vol. 145, pp. 172–177, Oct. 2019.
[11] W. Chu, B. Zhang, B. Liu, Z. Gui, and D. Zhao, "An optoelectronic targeting system for measuring the distribution of projectile motion based on the subdivision of a light screen," *Photonics*, vol. 126, pp. 1–13, Dec. 2020.
[12] D. Zhao, H. Zhou, J. Liu, B. Zhang, and Q. Luo, "High-precision velocity measuring system for projectiles based on retroreflective laser screen," *Optik*, vol. 124, no. 6, pp. 544–548, Mar. 2013.
[13] H. Tian, Y. Yuan, and D. Chen, "Improvement of the detection sensitivity uniformity of an indoor light screen array measurement system with large field of view angle using multi-lens splicing," *Optik*, vol. 181, pp. 971–977, Mar. 2019.
[14] W. Fan, J. Ni, H. Tian, and T. Yang, "Light transmission characteristics analyses of laserscreen in clear water based on Monte Carlo method," *Appl. Opt.*, vol. 59, no. 22, pp. 6625–6631, 2020.
[15] H. Li, Z. Wang, J. Gao, and Z. Lei, "Analysis and calculation object detection capture rate in multi-sky-screens across measurement system," *Optik*, vol. 124, no. 20, pp. 4369–4373, Oct. 2013.
[16] Y. Jiuqi, D. Tao, C. Ding, N. Jinping, and K. Baisheng, "Measurement method for fragment velocity based on active screen array in static detonation test," *Infr. Laser Eng.*, vol. 49, no. 1, pp. 206–212, 2020.
[17] X. Shang, P. Ma, and T. Chao, "Performance evaluation of electromagnetic railgun exterior ballistics based on cloud model," *IEEE Trans. Plasma Sci.*, vol. 45, no. 7, pp. 1614–1621, Jul. 2017.
[18] P. Ma, X. Shang, T. Chao, and M. Yang, "Simulation-based firing accuracy analysis for electromagnetic railgun with uncertainty," *IEEE Trans. Plasma Sci.*, vol. 47, no. 7, pp. 3358–3365, Jul. 2019.

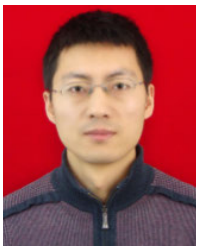

TAO DONG was born in Xi'an, Shaanxi, China, in 1980. He received the B.S. and M.S. degrees from Xi'an Technological University, in 2003 and 2006, respectively, and the Ph.D. degree in mechatronic engineering from the Xi'an University of Technology, in July 2015.

He is currently a Teacher with the School of Optoelectronic Engineering, Photoelectric Testing Technology Institute, Xi'an Technological University, where he is mainly studied design of optical machine structure for photoelectric detection instrument and photoelectric test technology for shooting range. He is a Doctor and an Associate Professor. He specializes in the overall design and performance analysis of optoelectronic testing instruments in Xi'an Technological University.

JIUQI YANG was born in Xi'an, Shaanxi, China, in 1994. He received the B.S. degree in science from Yanshan University, in 2016, and the M.S. degree in engineering from Xi'an Technological University, in 2020. He is currently a Researcher with the Shaanxi Province Key Laboratory of Photoelectric Measurement and Instrument Technology. His main research interest includes the measurement of external ballistic parameters of weapons.

DING CHEN (Member, IEEE) was born in Xi'an, Shaanxi, China, in 1982. He received the B.S. degree in electrical and information engineering, the M.S. degree in weapon systems and utilization engineering, and the Ph.D. degree in optical engineering from Xi'an Technological University, Shaanxi, in 2004, 2006, and 2020, respectively.

From 2010 to 2016, he was a Senior Engineer with the Radar Design and Research Institute, Xi'an Huang-he electromechanical Company, Ltd. Since 2020, he has been an Assistant Professor with the School of Armament Science and Technology, Xi'an Technological University. His research interests include photoelectric measurement and instrument technology, photoelectric information processing and acquisition, and radar/EW system design, simulation, and test. He is a member of SPIE, IET, and IEICE, and a Senior Member of the Chinese Institute of Electronics.

LINGQIU TAN was born in Xi'an, Shaanxi, China, in 1984. She received the B.S. and M.S. degrees in instruments science and technology, and the Ph.D. degree in mechanical engineering from the Xi'an University of Technology, in 2005, 2008, and 2016, respectively. Since 2016, she has been a Teacher with the School of Optoelectronic Engineering, Xi'an Technological University. She is currently involved in photoelectric detection instrument and photoelectric test technology for shooting range. She is a Doctor and a Lecturer. Her research interest includes photoelectric detection.